Efficient Classical Simulation of Spin Networks

by

Igor Andrade Sylvester

Submitted to the Department of Physics
in partial fulfillment of the requirements for the degree of

Bachelor of Science in Physics

at the

MASSACHUSETTS INSTITUTE OF TECHNOLOGY

June 2006

Author .....
Department of Physics
May 18, 2006

Certified by .....
Edward Farhi
Professor
Thesis Supervisor

Accepted by .....
David E. Pritchard
Senior Thesis Coordinator, Department of Physics

Efficient Classical Simulation of Spin Networks

by

Igor Andrade Sylvester

Submitted to the Department of Physics
on May 18, 2006, in partial fulfillment of the
requirements for the degree of
Bachelor of Science in Physics

Abstract

In general, quantum systems are believed to be exponentially hard to simulate using classical computers. It is in these hard cases where we hope to find quantum algorithms that provide speed up over classical algorithms. In the paradigm of quantum adiabatic computation, instances of spin networks with 2-local interactions could hopefuly efficiently compute certain problems in NP-complete [4]. Thus, we are interested in the adiabatic evolution of spin networks. There are analytical solutions to specific Hamiltonians for 1D spin chains [5]. However, analytical solutions to networks of higher dimensionality are unknown.

The dynamics of Cayley trees (three binary trees connected at the root) at zero temperature are unknown. The running time of the adiabatic evolution of Cayley trees could provide an insight into the dynamics of more complicated spin networks.

Matrix Product States (MPS) define a wavefunction anzatz that approximates slightly entangled quantum systems using poly(n) parameters. The MPS representation is exponentially smaller than the exact representation, which involves $O(2^n)$ parameters.

The MPS Algorithm evolves states in the MPS representation [3, 8, 2, 6, 10, 7]. We present an extension to the DMRG algorithm that computes an approximation to the adiabatic evolution of Cayley trees with rotationally-symmetric 2-local Hamiltonians in time polynomial in the depth of the tree. This algorithm takes advantage of the symmetry of the Hamiltonian to evolve the state of a Cayley tree exponentially faster than using the standard DMRG algorithm. In this thesis, we study the time-evolution of two local Hamiltonians in a spin chain and a Cayley tree.

The numerical results of the modified MPS algorithm can provide an estimate on the entropy of entanglement present in ground states of Cayley trees. Furthermore, the study of the Cayley tree explores the dynamics of fractional-dimensional spin networks.

Thesis Supervisor: Edward Farhi
Title: Professor

Acknowledgments

This thesis is the culmination of an Undergraduate Research Project Opportunity (UROP) that started one-and-half years ago in Spring 2005. I stopped by Professor Farhi's office and after a quick chat we agreed that I would attend his group meetings on Mondays. Since then I have attended most of the meetings and learned a whole lot of quantum information in the process. I would like to thank Eddie for letting me join his group, for providing me with invaluable insight into quantum physics and for his amusing sense of humor.

I would not have been able to complete this thesis without the help of Daniel Nagaj. We started working on the MPS algorithm after a month of my attending Eddie's group. Daniel helped me to understand the content of much of the material present in this thesis. While writing the simulation code, we both learned MATLAB tricks and, in a few ocassions, we spent long periods of time trying to find bugs. Daniel is a great physicist, teacher and friend.

The Physics department runs smoothly thanks to its amazing administrative staff. I would like to thank everyone in the Physics Education Office, specially Nancy Savioli.

Finally, I would like to thank my family for their infinite source of support. Thanks to my mother and my brother, I applied to MIT and made it through the past four years. I dedicate this thesis to them.

Contents

1 Introduction **11**
- 1.1 Quantum Computation . . . 11
- 1.2 Quantum Adiabatic Computation . . . 11
- 1.3 Matrix Product States . . . 12
- 1.4 Finding the Ground State of the QAH . . . 12
- 1.5 Quantum Adiabatic Evolution of Cayley Trees . . . 13
- 1.6 Outline . . . 13

2 Quantum Mechanics **15**
- 2.1 Postulates of Quantum Mechanics . . . 15
- 2.2 The Density Operator . . . 16
- 2.3 Composite Systems . . . 17
- 2.4 The Schmidt Decomposition . . . 17
- 2.5 An Illustrative Example of a Two-state System . . . 18

3 Matrix Product States **21**
- 3.1 The Matrix Product State Ansatz . . . 21
- 3.2 The Spin Chain . . . 22
- 3.3 An Illustrative Example of MPS . . . 28
- 3.4 The Cayley Tree . . . 29
- 3.5 Efficient Local Operations on Cayley Trees . . . 32

4 Simulation of Continuous-time Evolution **35**
- 4.1 The Runge-Kutta Approximation . . . 35
- 4.2 The Trotter Approximation . . . 35
- 4.3 Quantum Adiabatic Time Evolution . . . 36

5 Simulation Results **39**
- 5.1 The Spin Chain . . . 39
- 5.2 The Cayley Tree . . . 42

6 Conclusions and Future Work **43**

List of Figures

1-1 The 2-deep Cayley tree. The nodes represent spins and the edges correspond to interacting terms in the Hamiltonian. Deeper trees are built by gluing two spins to each peripheral node. 13

3-1 Application of a 2-local operator in the MPS representation. (a) Four spins with nearest-neighnor interactions. The spins in the two ends could be of higher dimensionality, in order to capture a bigger system of spins. (b) An entangling 2-local operation interacts the middle two spins. (c) The left half of the system is traced out. Effectively, half of the Hilbert space of the density matrix is traced over. (d) The MPS representation of the right-half of the system is restored by recomputing the Schmidt decomposition of the at the boundary. (e) The interacted system is represented entirely in the MPS representation by copying the reflection of the right side of the system into the left side. We are allowed to copy the Schmidt eigenvectors and eigenvalues because we assume that the system is reflection-symmetric. Note that this assumption excludes anti-symmetric states. 23

3-2 Two isolated spins in a spin chain. The letters a,b,c label the Schmidt eigenvectors corresponding to the bonds 1,2,3, respectively. 25

3-3 Application of a 3-local operator in the MPS representation. (a) Five spins interact locally. The two outermost spins maybe of higher dimensionality in order to capture the state of a longer spin chain. (b) An entangling unitary operator interacts the middle three spins; thus breaking the MPS representation of the state. (c) The three right-most spin states are traced out of the density matrix. (d) Alternatively, we trace out the two left-most spin states. (e) We compute the inner product of the density matrix in d with the reflection of the density matrix in c. We thus obtain the density matrix of the middle spin. (f) We recompute the MPS representation of the middle qubit. (g) The states of the second and fourth spins are found by computing the inner product of the state in f with the state in d. (h) The MPS representation of the interacted spin is reconstructed using the states in f and g. 27

3-4 Three isolated spins in a spin chain. The letters a,b,c,d label the Schmidt eigenstates of the bonds 1,2,3,4, respectively. 27

3-5 Primitive steps in the contraction a graph Cayley tree. Starting from the boundary of the tree, spins and bonds are traced succesively over until a single spin remains. A final trace over the spin states yields the inner product. 29

3-6 30

3-7 The Cayley tree explicitly showing the middle and first level qubits. Every spin and edge have an associated 3-rank tensor Γ and a Schmidt vector, respectively. The elements of these tensors and vectors are combined using the MPS recipe yo yield the wavefunction for the entire tree state. 31

3-8 A branch of a Cayley tree. Assuming that the operations depend only on the depth of the tree, the states of spins 2,3,4 are equal. Equivalently, the states of spins 5 and 6 are equivalent. 32

3-9 Operations on an efficient MPS representation of a Cayley tree. The goal is to interact all bonds once. Single-line represent bonds that have not been interacted while double-lines represent interacted bonds. (a) The state of the spins depends only on the depth. The circle with a number 1 inside represents the state of the middle spin in the first iteration of the algorithm. The square with a 1 represents the state of the spins in the second layer, in the first iteration, and so on. (b) The middle four spins are interacted in the MPS representation. The numbers are increased by 1 to indicate that they correspond to new states. (c) Three spins are interacted. (d) There is a square spin which has interacted all its bonds. Then, we copy the MPS Schmidt tensors and vectors to the other squares. (e) Another set of three spins is interacted. (f) The state of the triangle with all its bonds interacted is copied to the other triangle. We continue this process of interacting three spins and copying MPS parameters until we reach the end of the branch. 33

5-1 Lambda of middle bonds of AGREE on a spin chain. The parameters are $dt = 0.01$, $N = 10, \chi = 2$, and $T = 100$. 40
5-2 Normalized energy of AGREE on a spin chain for running times T. The parameters are $dt = 0.01, N = 10, \chi = 2$, and $T = 5 : 5 : 60$. 40
5-3 Probability of success of AGREE on a spin chain as a function of the running time T. The parameters are $dt = 0.01, N = 10, \chi = 2$. 41
5-4 Lambdas of middle bonds of instances of the FAVORITE problem on a spin chain for different ϵ. The parameters are $T = 50$, $dt = 0.1$, $X = 2$, $\epsilon = 0 : .02 : 1$. 41
5-5 Energy of AGREE on a Cayley tree. The parameters are $d = 20, T = 50, chi = 4$. . . 42
5-6 Lambdas of AGREE on a Cayley tree for different depths. The parameters are $d = 20, T = 40, \chi = 4$. 42

Chapter 1

Introduction

1.1 Quantum Computation

Quantum computers are a generalization of classical computers. Classical computers use bits to represent the state of computations, i.e. the value of a bit is either `0` or `1`. The basic operations on classical bits are, for example, the logical `OR`, `AND`, and `NOT`. On the other hand, quantum computers use qubits to represent the state of computations. A qubit $|\psi\rangle$ is a linear superposition of the computational basis states, i.e. $|\psi\rangle = a|0\rangle + b|1\rangle$. The operations that act on qubits are unitary gates.

We are concerned with efficient algorithms for solving hard problems. A problem is hard if the most efficient known algorithm takes a time that grows exponentially with the size of the problem. Similarly, an algorithm is efficient if it takes a time that grows polynomialy with the size of the problem.

R.P. Poplavskii (1975) and Richard Feynman (1982) suggested that classical computers are inherently inefficient at simulating quantum mechanical systems. That is, the time that a classical computer takes to simulate the evolution of a quantum system appears to be $O(2^n)$, where n is the dimension of the Hilbert space. However, Manin (1980) and Feynman (1982) suggested that quantum computers might be able to simulate quantum systems efficiently. This suggests that quantum computers have more computational power than classical computers.

1.2 Quantum Adiabatic Computation

Quantum computation has proven more efficient than classical computers at solving problems of searching and, possibly, factorization. These algorithms have been discovered using the circuit model of quantum computation. Similar to electrical circuits, the circuit model uses gates and wires to describe the steps of computations.

Another formulation of quantum computation is quantum adiabatic computation. The authors of [4] proposed a quantum algorithm to solve random instances of `3SAT`. However, they were unable to show that the algorithm runs efficiently for hard instances of the problem. Currently, there is no known efficient classical algorithm that solves hard instances of the satisfiability problem. The theorem states that if a system starts in its initial ground state and the time-dependence of the Hamiltonian is given by a parameter s which varies slowly in time, then the system will remain in the instantaneous ground state during the time evolution. For simplicity, we construct the time-dependent Hamiltonian, $\mathcal{H}(s)$, using a linear interpolation of the time-independent Hamiltonians $\mathcal{H}_B$, and $\mathcal{H}_P$, that is $\mathcal{H}(s) = (1-s)\mathcal{H}_B + s\mathcal{H}_P$, where $s = t/T$, and t varies from 0 (the beginning of the evolution) to T (the end of the evolution).

The adiabatic theorem gives an upper bound on the rate of change of the parameter s of the Hamiltonian such that the system remains in the instantaneous ground state. This lower bound corresponds to an upper bound on the evolution time T. The bound depends on the minimum

energy difference (energy gap) between the two lowest states of the adiabatic Hamiltonian.

The first step of an adiabatic quantum computation is to find an encoding to the solutions of a problem in the ground state of the problem Hamiltonian $\mathcal{H}_P$. Then, the system is slowly evolved from a known ground state of an arbitrary beginning Hamiltonian $\mathcal{H}_B$. The adiabatic theorem guarantees that, at the end of the evolution, the system is in the ground state of $\mathcal{H}_P$. Then, the solution to the problem is decoded from the ground state. The main question in adiabatic quantum computation is whether the minimum evolution time T grows exponentially with the size of the problem.

The theoretical computation of the energy gap is, in general, an open problem. Naively, we could find the eigenvalues of the Hamiltonian numerically. However, the Hamiltonian has $2^n \times 2^n$ elements, where n is the number of qubits. Therefore, we would need to keep track of approximately 2^n numbers to simulate the system. Practically, this problem becomes intractable for n of order 30.

In order to investigate the behavior of adiabatic evolutions in systems with hundreds of qubits, we approximate the state of n qubits using `poly(n)` numbers. Then, we search for the time for which the adiabatic algorithm finds the solution.

Aharonov and others have shown [1] that universal quantum computation is equivalent to quantum adiabatic computation with only nearest neighbor interactions. The central problem in quantum adiabatic computation [4] is to find the minimum energy gap between the ground state and the first excited state of the quantum adiabatic Hamiltonian (QAH) $\mathcal{H}(s) = (1-s)\mathcal{H}_B + s\mathcal{H}_P$. Here, $\mathcal{H}_B$ is the beginning Hamiltonian (whose ground state is easy to construct) and $\mathcal{H}_P$ is the problem Hamiltonian (whose ground state encodes the solution to a problem). Therefore, we are naturally interested in the quantum adiabatic evolution of spin networks.

1.3 Matrix Product States

The theoretical computation of the energy gap is, in general, an open problem. One could think of finding the eigenvalues of the Hamiltonian numerically. However, the Hamiltonian has $2^n \times 2^n$ elements, where n is the number of spins. Therefore, we would need to keep track of approximately $O(4^n)$ numbers to simulate the system. Practically, this problem becomes intractable for n of order 30.

Matrix product states (MPS) provide a approximate solution to the problem of simulating large, slightly entangled quantum systems. The approximate solution is possible only in systems with low entanglement. MPS do not work in highly entangled systems. The idea behind MPS is to write the state of a spin network in a basis that naturally accommodates entanglement. More specifically, we assign two $\chi \times \chi$ matrices to each spin (one matrix for each spin state) and a vector of length χ to each pair of interacting spins. Then, the amplitude of each basis state of the system is computed from the elements of the matrices and the vectors. Here, $\chi = 2^{\lceil n/2 \rceil}$ if we wish to represent the state exactly. However, if we choose $\chi = \mathtt{poly}(n)$, then the MPS anzatz gives an accurate description of slightly entangled states[1]. Therefore, MPS give a compact and accurate way of representing slightly entangled states using only $\mathtt{poly}(n)$ memory.

1.4 Finding the Ground State of the QAH

We will investigate two ways of finding the ground state of the quantum adiabatic Hamiltonian. The first method [2] involves simulating the time evolution of MPS states. Here, we use the Dyson series to expand the time evolution operator $T\exp(-i\int_0^t \mathcal{H}(t')\,dt')$ into a sequence of unitary operations involving only self or pairwise interactions. Then, the problem of evolving MPS states is reduced to applying local unitary gates. Since MPS states provide an efficient way of applying local gates, we can time evolve spin networks in time $\mathtt{poly}(n)$.

The expansion of the time evolution operator can be carried to high order. We investigate the dependence of the error in the simulation on the order of the expansion. Another method of finding

[1] This has been suggested by numerical simulations [9].

the ground state of the quantum adiabatic Hamiltonian is to evolve the state in imaginary time. In this case, we start by picking a time t and an admissible state. Then, we repeatedly apply $T\exp(-\int_0^t \mathcal{H}(t')\,dt')$ to the state. This has the effect of reducing the amplitudes of high-energy states; hence, this process increases the relative amplitude of the ground state.

1.5 Quantum Adiabatic Evolution of Cayley Trees

A Cayley tree consists of three binary trees connected at the root (see Figure 1-1). It is known [4] that, for the AGREE problem[2], i.e. an $\mathcal{H}_P$ for which the ground state is $\frac{1}{\sqrt{2}}(|0\rangle^{\otimes n} + |1\rangle^{\otimes n})$, the energy gap is $\Theta(1/n)$. Therefore, the adiabatic algorithm takes time $\mathtt{poly}(n)$. On the other hand, the adiabatic algorithm fails for a two-dimensional lattice because the energy gap is small. So, it is interesting to investigate the behavior of the adiabatic algorithm in Cayley trees, which can be thought of being a structure in between a line and a lattice.

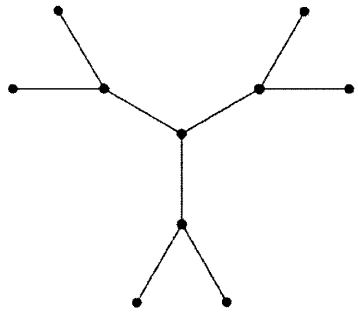

Figure 1-1: The 2-deep Cayley tree. The nodes represent spins and the edges correspond to interacting terms in the Hamiltonian. Deeper trees are built by gluing two spins to each peripheral node.

1.6 Outline

This thesis builds the necessary tools to simulate adiabatic time evolution in spin networks. For the purposes of this thesis, spin networks are collection of spins-1/2 particles with pair-wise interactions. We build on the principles of quantum mechanics taught at the undergraduate level. The introductory chapter presents the theoretical tools needed to understand matrix product states (MPS). These include the density operator and the Schmidt decomposition.

Chapter 3 elaborates on MPS in the context of the finite spin chain. We derive the MPS anzatz and explain how to act on the state with local operations. The chapter ends with an example MPS state. Chapter 4 Chapter 5 combines the results of the previous two chapters to give algorithms to simulate time evolution of spin networks. We provide a novel algorithm that simulates a class of spin networks in time $O(\log(n))$, where n is the number of spins in the network. This is an improvement on the running time of the MPS algorithm, which runs in time $O(n)$. Chapter 6 summarizes conclusions and future work.

[2] $\mathcal{H}_P = \sum_{i=1}^{n}(1 - \sigma_Z^{(i)} \otimes \sigma_Z^{(i+1)})$, with $i+1$ identified with 1.

Chapter 2

Quantum Mechanics

2.1 Postulates of Quantum Mechanics

Quantum mechanics (QM) is a theory of physical systems. The theory of QM is defined by postulates. We review the postulates of QM in this section.

State Space

The first postulate of QM says that the state of a system is completely described, up to a global phase factor, by a state vector ket $|\psi\rangle$. Hence, if a system is described by $|\psi\rangle$ then the system is equivalently described by $e^{i\phi}|\psi\rangle$, where ϕ is a real constant.

The system is allowed to be in any state $|\psi\rangle$ that belongs to the system's Hilbert space $\mathcal{H}$. The Hilbert space $\mathcal{H}_d$ is characterized by its dimension d. The smallest Hilbert space $\mathcal{H}_2$ has dimension 2 and corresponds to the quantum spin-1/2, which is also known as the qubit.

For each state ket $|\psi\rangle$ there is a dual state bra $\langle\psi|$. The inner product between two states $\langle\psi|\,\phi\rangle$ is a complex number.

When performing computations, it is convenient to represent state kets using vectors. The Hilbert space corresponds to the space of vectors of complex numbers.

Measurement

The second postulate of QM concerns physical observables. For any physical observable $\mathcal{M}$ there is an associated Hermitian operator M which acts on state kets. The eigenkets of $\mathcal{M}$ are defined to be the kets that satisfy $M|m\rangle = m|m\rangle$, where m is the eigenvalue of M that corresponds to the ket $|m\rangle$. The real-valued eigenvalue m is the value of the measured observable M.

How do measurement operators act on more general states? Given an observable $\mathcal{M}$, the eigenkets of $\mathcal{M}$ form a basis for the Hilbert space. Thus, we may expand any state $|\psi\rangle$ in terms of the observable eigenkets:

$$M|\phi\rangle = M\sum_m \langle m|\,\phi\rangle\,|m\rangle \tag{2.1}$$

$$= \sum_m \langle m|\,\phi\rangle\, m\,|m\rangle\,. \tag{2.2}$$

After the measurement of the observable $\mathcal{M}$, quantum mechanics postulates that the state $|\phi\rangle$ collapses into one of the eigenkets $|m\rangle$ with probability $|\langle m|\,\phi\rangle|^2$.

Time Evolution

The last postulate of QM states that the time evolution of a system described by $|\psi(t)\rangle$ is given by a time evolution unitary operator U and acts on state kets as:

$$|\psi(t)\rangle = U(t, t_0)\,|\psi(t_0)\rangle\,. \tag{2.3}$$

The operator $U(t, t_0)$ evolves kets from time t_0 to t. Enforcing the property of composition on U gives rise to the Schrödinger equation:

$$i\hbar\frac{\partial}{\partial t}\,|\Psi(t)\rangle = H(t)\,|\Psi(t)\rangle\,, \tag{2.4}$$

where $\hbar$ is Planck's constant and $i^2 = -1$. Here, the time-dependent operator $H(t)$ is the Hamiltonian of the system. The Hamiltonian is the physical observable of the energy. For convenience, in the remainder of this thesis, we set $\hbar = 1$.

The solution to the Schrödinger equation (2.4) is trivial if the state ket is an eigenstate of the Hamiltonian and the Hamiltonian commutes with itself at different times. That is, if $H\,|\Psi(t)\rangle = E\,|\Psi(t)\rangle$, and $[H(t_0), H(t_1)] = 0$ for any t_0 and t_1, the solution is given by

$$|\Psi(t)\rangle = e^{-iE_n(t-t_0)}\,|\Psi(t_0)\rangle\,, \tag{2.5}$$

where $|\psi(t_0)\rangle$ is specified by the initial conditions of the system.

If the time evolution of a state ket that is not an eigenstate of the Hamiltonian is easily derived from Eq. 2.5. If we continue to assume that the Hamiltonian commutes with itself at later times, then the time evolution of any state ket is given by

$$|\Psi(t)\rangle = \sum_n e^{-iE_n(t-t_0)}\,|n\rangle\,\langle n|\,\Psi(t_0)\rangle\,, \tag{2.6}$$

where $\{|n\rangle\}$ is the set of energy eigenvectors, i.e. $H\,|n\rangle = E_n\,|n\rangle$.

More generally, if the Hamiltonian does not commute with itself at later times, then the time evolution operator is given by the Dyson series

$$U(t+\Delta t, t) = 1 + \sum_{n=1}^{\infty}(-1)^n \int_t^{t+\Delta t} dt_1 \int_t^{t_1} dt_2 \ldots \int_t^{t_{n-1}} dt_n H(t_1)H(t_2)\ldots H(t_n). \tag{2.7}$$

2.2 The Density Operator

The density operator is an alternative representation for the state of quantum systems. By definition, the density operator of a system is given by

$$\rho = |\psi\rangle\,\langle\psi|\,, \tag{2.8}$$

where $|\psi\rangle$ is the state ket that describes the system. The density matrix is the matrix-representation of the density operator in a particular basis. We will use the terms density operator and density matrix interchangibly and use the computational basis by default. It turns out that we can reformulate the postulates of QM in terms of the density matrix:

1. The time-evolution of the density matrix is given by $\rho(t) = U\rho U^\dagger$, where U is the time-evolution operator.

2. For every observable $\mathcal{M}$ there is a set of projection matrices $\{M_m\}$, where m labels the outcome of the measurement. After a measurement described by M_m, the density matrix collapses to

$$\rho \Rightarrow \frac{M_m\rho M_m^\dagger}{\mathrm{Tr}(M_m^\dagger M_m\rho)} = \frac{M_m\rho M_m}{\mathrm{Tr}(M_m^2\rho)}, \tag{2.9}$$

with probability $p(m) = \mathrm{Tr}(M_m^\dagger M_m \rho)$. The last equality follows from the fact that the projection matrices are Hermitian ($M_m = M_m^\dagger$) and from the cyclic property of the trace operator.

The density matrix is a more powerful descriptions of quantum systems than the state ket representations. The density matrix can describe mixed states. A quantum system is in a mixed state if we know that the system is in one of the states $\{|\psi_1\rangle, |\psi_2\rangle \ldots |\psi_k\rangle\}$ with probabilities $\{p_1, p_2 \ldots p_k\}$, where $\sum_i p_i = 1$. In this case, the density matrix is defined as

$$\rho = \sum_i p_i |\psi_i\rangle \langle\psi_i| . \tag{2.10}$$

2.3 Composite Systems

We can compose quantum systems to form larger systems. For example, given two qubits A and B each with Hilbert space $\mathcal{H}_1$, we can form the system $A \otimes B$ with Hilbert space $\mathcal{H}_1 \otimes \mathcal{H}_1 = \mathcal{H}_1^{\otimes 2}$, where $\otimes$ is read "tensor."

We obtain the density operator of a component of the system by tracing over the rest of the system. More concretely, the density matrix of qubit A is given by

$$\rho_A = \mathrm{Tr}_B(\rho), \tag{2.11}$$

where Tr_B is the partial trace over system B. The partial trace is defined on pure states as

$$\mathrm{Tr}_B(\rho) = \mathrm{Tr}_B(\rho_A \otimes \rho_B) = \rho_A \otimes \mathrm{Tr}(\rho_B). \tag{2.12}$$

For convenience, we will drop the $\otimes$ notation in the remainder of this thesis.

2.4 The Schmidt Decomposition

The Schmidt decomposition is a useful representation for a pure state of a composite system in terms of pure states of its constituents. More explicitly, if a bipartite system AB is in the state $|\psi\rangle$ then the state may be written in terms of pure states of systems A and B, respectively:

$$|\psi\rangle = \sum_{i=1}^{\chi} \lambda_i |A_i\rangle |B_i\rangle . \tag{2.13}$$

Here, $|A_i\rangle$ and $|B_i\rangle$ are called the Schmidt eigenvectors of the system AB. The Schmidt eigenvalues λ_i are non-negative and satisfy $\sum_i \lambda_i^2 = 1$. The number of non-zero Schmidt eigenvalues, χ, is called the Schmidt number. We will obtain the dependence of χ on the the system AB and show that $\chi \leq 2^{m/2}$, where m is the smallest numerber of qubits of the systems A and B.

We now derive the Schmidt decomposition. First, let's consider the case where both the systems A and B have dimension d. Later we will generalize to the case of different dimensions. Let $\{|j\rangle\}$ and $\{|k\rangle\}$ be bases for the systems A and B, respectively. Then, the state $|\psi\rangle$ may be written

$$|\psi\rangle = \sum_{j=1}^{d} \sum_{k=1}^{d} a_{jk} |j\rangle |k\rangle , \tag{2.14}$$

for some matrix a of complex numbers a_{jk}. We can rewrite the matrix elements a_{jk} as

$$a_{jk} = \sum_{i=1}^{d} u_{ji} d_{ii} v_{ik}, \tag{2.15}$$

where d is a diagonal matrix, and u and v are unitary matrices. Then, we can write

$$|\psi\rangle = \sum_{i=1}^{d}\sum_{j=1}^{d}\sum_{k=1}^{d} u_{ji} d_{ii} v_{ik} |j\rangle |k\rangle . \tag{2.16}$$

The last step is to define the Schmidt eigenvectors

$$\begin{aligned} |i_A\rangle &\equiv \sum_j u_{ji} |j\rangle \\ |i_B\rangle &\equiv \sum_k v_{ik} |k\rangle \end{aligned}$$

and the Schmidt eigenvalues $\lambda_i = d_{ii}$. Using these definitions, we obtain

$$|\psi\rangle = \sum_{i=1}^{d} \lambda_i |i_A\rangle |i_B\rangle . \tag{2.17}$$

Since basis $\{|j\rangle\}$ is orthonormal and the matrix u is unitary, the Schmidt vectors $\{|i_A\rangle\}$ form an orthonormal set. This also applies to the set $\{|i_B\rangle\}$.

We now consider the case where the sub-systems A and B have different dimensions. Without loss of generality, we can assume that systems A and B have dimensions a and b, with $a > b$.

How do we compute the Schmidt eigenvalues and eigenvectors? For computational purposes, it is convenient to switch to the density operator representation of states. First, we present the algorithm to compute the Schmidt decomposition and then we analyze its correctness.

Let us consider the simple example of computing the Schmidt decomposition for the bipartite system discussed earlier. We proceed as follows:

1. Compute the density matrix of the system AB: $\rho = |\psi\rangle \langle\psi|$.
2. Obtain the mixed-state reduced density matrix for the system A by tracing over system B: $\rho_A = \mathrm{Tr}_B(\rho)$.
3. Diagonalize the reduced density matrix ρ_A. This corresponds to computing the normalized eigenvectors $\{|i_A\rangle\}$ of ρ_A, which are the Schmidt eigenvectors of the system AB.
4. Find the Schmidt eigenvalues by computing the inner product $\lambda_i = \langle i_A i_B| \Psi\rangle$.

2.5 An Illustrative Example of a Two-state System

For pedagogical reasons we compute the Schmidt decomposition of the EPR state

$$|\psi\rangle = \frac{1}{\sqrt{2}}(|00\rangle + |11\rangle).$$

We follow the algorithm given in the previous section. The density matrix of the EPR pair is

$$\begin{aligned} \rho &= |\psi\rangle \langle\psi| \\ &= \frac{1}{4}(|00\rangle + |11\rangle)(\langle 00| + \langle 11|) \\ &= \frac{1}{4}(|00\rangle \langle 00| + |00\rangle \langle 11| + |11\rangle \langle 00| + |11\rangle \langle 11|). \end{aligned}$$

The reduced density matrix of system A is given by

$$\rho_A = \mathrm{Tr}_B(\rho)$$

$$= \frac{1}{4}\mathrm{Tr}_B(|00\rangle\langle 00| + |00\rangle\langle 11| + |11\rangle\langle 00| + |11\rangle\langle 11|).$$

In order to evaluate the partial trace, we note that $|00\rangle\langle 00| = |0\rangle\langle 0| \otimes |0\rangle\langle 0|$. Hence,

$$\mathrm{Tr}(|00\rangle\langle 00|) = |0\rangle\langle 0| \otimes \langle 0|\, 0\rangle\,.$$

Thus, we obtain

$$\rho_A = \frac{1}{4}(|0\rangle\langle 0| \otimes \langle 0|\, 0\rangle + |0\rangle\langle 1| \otimes \langle 0|\, 1\rangle + |1\rangle\langle 0| \otimes \langle 1|\, 0\rangle + |1\rangle\langle 1| \otimes \langle 1|\, 1\rangle).$$

By the orthonormality of the computational basis,

$$\rho_A = \frac{1}{4}(|0\rangle\langle 0| + |1\rangle\langle 1|).$$

The two Schmidt eigenvectors are given by the eigenvectors of ρ_A:

$$\begin{aligned} |1_A\rangle &= |1_B\rangle = |0\rangle \\ |2_A\rangle &= |2_B\rangle = |1\rangle\,. \end{aligned}$$

We verify that the Schmidt eigenvectors indeed form an orthonormal set. The Schmidt eigenvalues are given by the inner producrs:

$$\begin{aligned} \lambda_1 &= \langle 1_A 1_B|\, \psi\rangle = 1/\sqrt{2} \\ \lambda_2 &= \langle 2_A 2_B|\, \psi\rangle = 1/\sqrt{2} \end{aligned}$$

We verify that the Schmidt eigenvalues satisfy $\sum_i \lambda_i^2 = 1$.

The EPR pair has two non-zero Schmidt eigenvalues, therefore $\chi = 2$. This is the maximum for two two-state systems because $\chi \leq 2^{m/2}$, where m is the dimensionality of the sub-systems. Since χ gives a measure of entanglement, we say that the EPR pair is maximally entangled.

Chapter 3

Matrix Product States

In simple terms, matrix product states (MPS) are a generalization to the Schmidt decomposition. The Schmidt decomposition is a description of a system using states of two of its subsystems that shows the role of entanglement between the subsystems. When there is little entanglement, the Schmidt decomposition has only a few terms. MPS provide a compact representation for slightly entangled systems, where we treat each qubit as a subsystem. We will exploit this representation to efficiently simulate slightly entangled systems.

In Section 3.1 we derive the MPS ansatz for a spin chain. Section 3.2 develops algorithms for applying 1-,2-, and 3-local unitary operations and computing expectation values in a spin chain. Finally, Section 3.4 extends the MPS representation to Cayley trees.

3.1 The Matrix Product State Ansatz

The MPS Ansatz generalizes the Schmidt decomposition for multi-partite systems. Let's consider a system composed of n qubits. The state of the system is given by

$$|\Psi\rangle = \sum_{i_1=0}^{1} \cdots \sum_{i_n=0}^{1} C_{i_1 \ldots i_n} |i_1\rangle \ldots |i_n\rangle , \tag{3.1}$$

where the coefficients $C_{i_1 \ldots i_n}$ are the matrix elements of $|\psi\rangle$ in the computational basis. The MPS ansatz consists of expressing

$$C_{i_1 \ldots i_n} = \sum_{\alpha_1=1}^{\chi_1} \sum_{\alpha_2=1}^{\chi_2} \cdots \sum_{\alpha_n=1}^{\chi_n} \Gamma^{[1]i_1}_{\alpha_1} \lambda^{[1]}_{\alpha_1} \Gamma^{[2]i_2}_{\alpha_1 \alpha_2} \lambda^{[2]}_{\alpha_2} \Gamma^{[3]i_3}_{\alpha_2 \alpha_3} \ldots \Gamma^{[n]i_n}_{\alpha_{n-1}} . \tag{3.2}$$

Here, $\Gamma^{[1]i_1}_{\alpha_1}$ and $\lambda^{[1]}_{\alpha_1}$ are the Schmidt eigenvectors and eigenvalues for the partition $1 : 2 \ldots n$, respectively. Similarly, the other Γ's and λ's are the correspond to the Schmidt decompositions of successive partitions. The Schmidt number χ_i corresponds to the parition at the i-th bond. Now, for a bipartite system AB, where the Schmidt number $\chi \leq 2^{\lceil min(|A|,|B|)/2 \rceil}$, where $|A|$ and $|B|$ are the number of spins in systems A and B, respectively. Therefore, we have $\chi_i \leq 2^{\lceil i/2 \rceil}$. If this constraint is satisfied by equality, we say that the system in maximally entangled.

Numerical simulations have shown that the Schmidt eigenvalues are exponentially small in the Schmidt number for slightly entangled spin chains [9]. Therefore, the MPS anzatz becomes a good approximation for these systems if we truncate the representation to χ =poly(n).

Let us derive the MPS anzatz to better understand it. The Schmidt decomposition $1 : 2 \ldots n$ is

$$|\Psi\rangle = \sum_{\alpha_1}^{\chi_1} \left| \Phi^{[1]}_{\alpha_1} \right\rangle \lambda^{[1]}_{\alpha_1} \left| \Phi^{[2 \ldots]}_{\alpha_1} \right\rangle , \tag{3.3}$$

where χ_1 is the Schmidt number, $\lambda^{[1]}_{\alpha_1}$ are the Schmidt eigenvalues indexed by α_1, and $\left|\Phi^{[1]}_{\alpha_1}\right\rangle$ and $\left|\Phi^{[2\ldots n]}_{\alpha_1}\right\rangle$ are the Schmidt basis states for systems 1 and $2\ldots n$. We proceed by expressing the Schmidt vector corresponding to qubit 1 in the computational basis:

$$|\Psi\rangle = \sum_{i_1=0}^{1}\sum_{\alpha_1=1}^{\chi_1} \Gamma^{[1]i_1}_{\alpha_1}\lambda^{[1]}_{\alpha_1}|i_1\rangle \left|\Phi^{[2\ldots n]}_{\alpha_1}\right\rangle. \tag{3.4}$$

Now we repeat the Schmidt decomposition for the system $2:3\ldots n$ and express the Schmidt eigenvectors of qubit 2 in the computational basis:

$$|\Psi\rangle = \sum_{i_1=0}^{1}\sum_{\alpha_1=1}^{\chi_1}\sum_{i_2=0}^{1}\sum_{\alpha_2=1}^{\chi_2} \Gamma^{[1]i_1}_{\alpha_1}\lambda^{[1]}_{\alpha_1}\Gamma^{[2]i_2}_{\alpha_1\alpha_2}\lambda^{[2]}_{\alpha_2}|i_1\rangle|i_2\rangle \left|\Phi^{[3\ldots n]}_{\alpha_2}\right\rangle. \tag{3.5}$$

We can repeat this process qubit by qubit until we obtain the MPS anzatz:

$$|\Psi\rangle = \sum_{i_1=0}^{1}\cdots\sum_{i_n=0}^{1}\sum_{\alpha_1=1}^{\chi_1}\cdots\sum_{\alpha_n=1}^{\chi_n} \Gamma^{[1]i_1}_{\alpha_1}\lambda^{[1]}_{\alpha_1}\Gamma^{[2]i_2}_{\alpha_1\alpha_2}\lambda^{[2]}_{\alpha_2}\Gamma^{[3]i_3}_{\alpha_2\alpha_3}\cdots\Gamma^{[n]i_n}_{\alpha_{n-1}}|i_1\rangle\ldots|i_n\rangle. \tag{3.6}$$

3.2 The Spin Chain

Expectation Values

The expectation of σ_X is given by

$$\begin{aligned}\langle\Psi|\,\sigma^{[2]}_X\,|\Psi\rangle &= \sum_{b'\,c'}\sum_{j'}\sum_{b\,c}\sum_{j}(\lambda^{[2]}_{b'})^*(\Gamma^{[2],j'}_{b'c'})^*(\lambda^{[3]}_{c'})^*\lambda^{[2]}_{b}\Gamma^{[2],j}_{bc}\lambda^{[3]}_{c}\,\langle j'|\,\sigma_X\,|j\rangle\,\langle b'\,c'|\,b\,c\rangle &(3.7)\\ &= \sum_{j'}\sum_{j}\mathrm{Tr}\left((\Lambda^{[2]}\Gamma^{[2],j'}\Lambda^{[3]})^\dagger(\Lambda^{[2]}\Gamma^{[2],j}\Lambda^{[3]})\right)\langle j'|\,\sigma_X\,|j\rangle, &(3.8)\end{aligned}$$

where $\Xi_{[2],i} = \Lambda^{[2]}\Gamma^{[2],i}\Lambda^{[3]}$. In the computational basis,

$$\langle\Psi|\,\sigma^{[2]}_X\,|\Psi\rangle = \mathrm{Tr}(\Xi^\dagger_{[2],0}\Xi_{[2],1} + \Xi^\dagger_{[2],1}\Xi_{[2],0}). \tag{3.9}$$

The expectation of $\sigma_Z\otimes\sigma_Z$ is given by

$$\begin{aligned}\langle\Psi|\,\sigma^{[1]}_Z\otimes\sigma^{[2]}_Z\,|\Psi\rangle &= \sum_{i'\,j'}\sum_{i\,j}\mathrm{Tr}\left((\Lambda^{[1]}\Gamma^{[1],i'}\Lambda^{[2]}\Gamma^{[2],j'}\Lambda^{[3]})^\dagger(\Lambda^{[1]}\Gamma^{[1],i}\Lambda^{[2]}\Gamma^{[2],j}\Lambda^{[3]})\right)\langle i'\,j'|\,\sigma_Z\otimes\sigma_Z\,|i\,j\rangle &(3.10)\\ &= \sum_{i'\,j'}\sum_{i\,j}\Xi^\dagger_{[1,2],i'j'}\Xi_{[1,2],ij}\,\langle i'\,j'|\,\sigma_Z\otimes\sigma_Z\,|i\,j\rangle, &(3.11)\end{aligned}$$

where $\Xi_{[1,2],ij} = \Lambda^{[1]}\Gamma^{[1],i}\Lambda^{[2]}\Gamma^{[2],j}\Lambda^{[3]}$. In the computational basis,

$$\langle\Psi|\,\sigma^{[1]}_Z\otimes\sigma^{[2]}_Z\,|\Psi\rangle = \mathrm{Tr}(\Xi^\dagger_{[1,2],00}\Xi_{[1,2],00} - \Xi^\dagger_{[1,2],10}\Xi_{[1,2],10} - \Xi^\dagger_{[1,2],01}\Xi_{[1,2],01} + \Xi^\dagger_{[1,2],11}\Xi_{[1,2],11}). \tag{3.12}$$

1-local Unitary Operators

The MPS anzatz is particularly efficient for applying local operators such as σ_X and $\sigma_Z\sigma_Z$. Local means that the operator acts on a constant number of neighboring bits—independent of the size of the system. Let's compute the actions of 1-local and 2-local unitary operators on a general MPS.

The 1-local unitary operator $U = \mathcal{I}_1\otimes\ldots\otimes U_k\otimes\mathcal{I}_n$ acts on the k-th qubit with U_k and trivially on the remaining qubits. How does the MPS representation of the state $|\psi\rangle$ change? If the original

state is given by the MPS

$$|\psi\rangle = \sum_{i=0}^{1} \sum_{a,b=1}^{\chi} \left|\Phi_a^{[1\ldots k-1]}\right\rangle \lambda_a^{[k-1]} \left(\Gamma_{ab}^{[k]i} |i\rangle\right) \lambda_b^{[k]} \left|\Phi_b^{[k+1\ldots n]}\right\rangle , \tag{3.13}$$

then the new state is given by

$$|\psi'\rangle = \sum_{i=0}^{1} \sum_{a,b=1}^{\chi} \left|\Phi_a^{[1\ldots k-1]}\right\rangle \left(\Gamma'^{[k]i}_{ab} |i\rangle\right) \left|\Phi_c^{[k+1\ldots n]}\right\rangle . \tag{3.14}$$

where

$$\Gamma'^{[k]i_k}_{\alpha_{k-1}\alpha_k} = \sum_{a,b} (U_k)^{ab}_{\alpha_{k-1}\alpha_k} \Gamma^{[k]i_k}_{ab} . \tag{3.15}$$

Here, χ is the maximum Schmidt number of all the partitions of the qubits. All the other Γ's and λ's remain unchanged. Note that 1-local operations do not change the structure of the MPS anzatz. This is not true for 2-local operations.

2-local Unitary Operators

The application of 1-local operators in the MPS representation is trivial because there spin states are not entangled. However, 2-local operations may entangle two spins. See Figure 3-1 for a diagrammatic description of the application of 2-local operators in the MPS representation. The 2-local

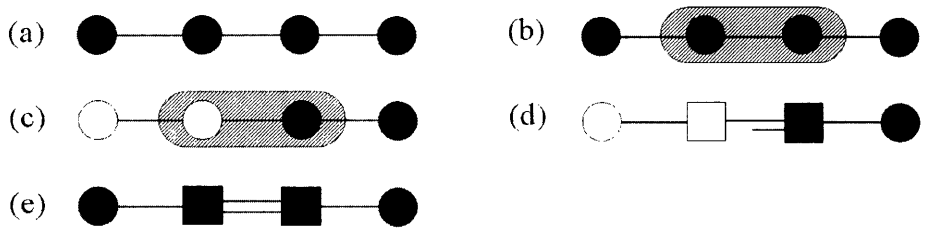

Figure 3-1: Application of a 2-local operator in the MPS representation. (a) Four spins with nearest-neighnor interactions. The spins in the two ends could be of higher dimensionality, in order to capture a bigger system of spins. (b) An entangling 2-local operation interacts the middle two spins. (c) The left half of the system is traced out. Effectively, half of the Hilbert space of the density matrix is traced over. (d) The MPS representation of the right-half of the system is restored by recomputing the Schmidt decomposition of the at the boundary. (e) The interacted system is represented entirely in the MPS representation by copying the reflection of the right side of the system into the left side. We are allowed to copy the Schmidt eigenvectors and eigenvalues because we assume that the system is reflection-symmetric. Note that this assumption excludes anti-symmetric states.

unitary operator $U = \mathcal{I}_1 \otimes \ldots \otimes U_{k,k+1} \otimes \ldots \mathcal{I}_n$ acts on the k-th and $(k+1)$-th qubits with U_k and trivially on the remaining qubits. For convenience, we assume that U_k acts on neighboring qubits. If this were not the case, then we could peform `SWAP` operations that brought two distant qubits together; then, act with the operator, and finally undo the `SWAP` sequence to bring the qubits to their natural order. The original state is given by

$$\begin{aligned} |\Psi\rangle &= \sum_{i,j=0}^{1} \sum_{a,b,c=1}^{\chi} \left|\Phi_a^{[1\ldots k-1]}\right\rangle \left(\lambda_a^{[k-1]} \Gamma_{ab}^{[k]i} \lambda_b^{[k]} \Gamma_{bc}^{[k+1]j} \lambda_a^{[k-1]} |i\rangle |j\rangle\right) \left|\Phi_a^{[k+2\ldots n]}\right\rangle \\ &= \sum_{i,j=0}^{1} \sum_{a,b,c=1}^{\chi} \Theta_{ac}^{ij} |a\rangle |i\rangle |j\rangle |c\rangle , \end{aligned}$$

where

$$\begin{aligned} |a\rangle &= \lambda_a^{[k-1]} \left|\Phi_a^{[1\ldots k-1]}\right\rangle, \\ |c\rangle &= \lambda_c^{[k+1]} \left|\Phi_c^{[k+2\ldots n]}\right\rangle, \\ \Theta_{ac}^{ij} &= \Gamma_{ab}^{[k]i} \lambda_b^{[k]} \Gamma_{bc}^{[k+1]j}. \end{aligned}$$

Then the new state is given by

$$|\Psi'\rangle = \sum_{i,j=0}^{1} \sum_{a,b,c=1}^{\chi} \Theta'^{ij}_{ac} |aijc\rangle, \tag{3.16}$$

where

$$\Theta'^{ij}_{ac} = (U_k)^{ij}_{a'c'} \Theta^{ij}_{ac}. \tag{3.17}$$

We see that the MPS representation has been broken because the state (3.16) cannot immediately be written as an MPS anzatz (Eq. 3.6). We wish to write

$$\Theta'^{ij}_{ac} = \Gamma'^{[k]i}_{ab} \lambda'^{[k]}_{b} \Gamma'^{[k+1]j}_{bc}, \tag{3.18}$$

where the primed quantities indicate the parameters describing the new state. We fix the representation by re-computing the Schmidt decomposition of the partition $1 \ldots k : k+1 \ldots n$. The following algorithm expresses the state (3.16) as an MPS:

1. Compute the density matrix of the new state

$$\begin{aligned} \rho &= |\psi'\rangle \langle\psi'| & (3.19) \\ &= \sum_{i,j,i',j'=0}^{1} \sum_{a,b,c,a',b',c'=1}^{\chi} \Theta^{ij}_{ac} \left(\Theta^{i'j'}_{a'c'}\right)^* |aijc\rangle \langle a'i'j'c'|. & (3.20) \end{aligned}$$

2. Perform a partial trace over qubits $1 \ldots k$: $\rho^{[k+1\ldots n]} = \mathrm{Tr}_{1\ldots k}\rho$

3. Diagonalize $\rho^{[k+1\ldots n]}$ and compute its eigenvectors.

4. Find the basis $|a\rangle$ for the space of qubits $k+1 \ldots n$ by computing the inner product $|a\rangle = \langle m|\ \psi\rangle$, where $|m\rangle$ are the eigenvectors of $\rho^{[1\ldots k]}$.

5. Update the MPS representation using the bases $|m\rangle$ and $|a\rangle$.

Details of the Algorithm

The computational basis states of spins 1 and 2 are labelled $|i\rangle$ and $|j\rangle$, respectively. The basis states for the system left to spin 1 and the system to the right of spin 2 are labelled $|\alpha_a\rangle$ and $|\beta_c\rangle$, respectively. The bonds are labelled 1,2, and 3. The system is partitioned into a left part (L) and a right part (R). The indices a, b and c label Schmidt terms.

After the time-evolution of spins i and j, the state of the system is

$$\begin{aligned} |\Psi\rangle &= \sum_{a\,b\,c} \sum_{i\,j} \sum_{r\,s} U^{(ij)}_{(rs)} \lambda_a^{[1]} \Gamma_{ab}^{[1],r} \lambda_b^{[2]} \Gamma_{bc}^{[2],s} \lambda_c^{[3]} |\alpha_a\, i\, j\, \beta_c\rangle & (3.21) \\ &= \sum_{a\,c} \sum_{i\,j} \Theta_{(ai)(cj)} |\alpha_a\, i\, j\, \beta_c\rangle, & (3.22) \end{aligned}$$

where U^{ij}_{rs} is a unitary operator on spins 1 and 2. The spin indices are summed over $\{0, 1\}$ and the

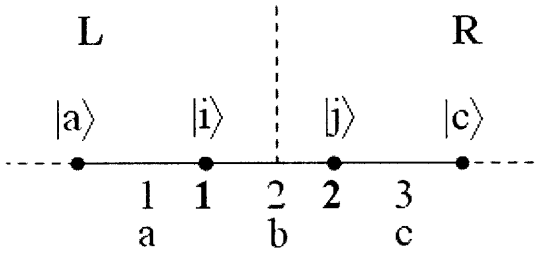

Figure 3-2: Two isolated spins in a spin chain. The letters a,b,c label the Schmidt eigenvectors corresponding to the bonds 1,2,3, respectively.

Schimdt indices are summer over $\{1 \ldots \chi\}$; and

$$\Theta_{(ai)(cj)} = \sum_b \sum_{r\,s} U^{(ij)}_{(rs)} \lambda^{[1]}_a \Gamma^{[1],r}_{ab} \lambda^{[2]}_b \Gamma^{[2],s}_{bc} \lambda^{[3]}_c. \tag{3.23}$$

In matrix notation,

$$\Theta = U \Lambda^{[1]} \Gamma^{[1]} \Lambda^{[2]} \Gamma^{[2]} \Lambda^{[3]}, \tag{3.24}$$

where $\Lambda^{[\ell]} = \mathrm{diag}(\lambda^{[\ell]})$. The density matrix is

$$\begin{aligned} \rho &= |\Psi\rangle\langle\Psi| \\ &= \sum_{a\,c} \sum_{i\,j} \sum_{a'\,c'} \sum_{i'\,j'} \Theta_{(ai)(cj)} \Theta^*_{(a'i')(c'j')} |\alpha_a\, i\, j\, \beta_c\rangle \langle \alpha'_a\, i'\, j' \beta'_c| . \end{aligned} \tag{3.25}$$

The reduced density matrix for the left partition is

$$\begin{aligned} \rho_L &= \mathrm{Tr}_R(\rho) \\ &= \sum_{c''} \sum_{j''} \sum_{a\,b} \sum_{i\,j} \sum_{a'\,c'} \sum_{i'\,j'} \Theta_{(ai)(cj)} \Theta^*_{(a'i')(c'j')} \langle j''\, \beta_{c''}|\, j\, \beta_c\rangle\, |\alpha_a\, i\rangle \langle \alpha_{a'}\, i'|\, \langle j' \beta_{c'}|\, j''\, \beta_{c''}\rangle \\ &= \sum_{a\,c} \sum_{i\,j} \sum_{a'\,c'} \sum_{i'} \Theta_{(ai)(cj)} \Theta^*_{(a'i')(cj)} |\alpha_a\, i\rangle \langle \alpha_{a'} i'| \end{aligned} \tag{3.26}$$

Hence, in the $|\alpha\, i\rangle$ basis,

$$\rho_L = \Theta\Theta^\dagger, \tag{3.27}$$

where $\dagger$ denotes the hermitian conjuage operation (i.e. non-complex-conjugate matrix transpose followed by complex conjugation). Similarly,

$$\begin{aligned} \rho_R &= \mathrm{Tr}_L(\rho) \\ &= \sum_{a''} \sum_{i''} \sum_{a\,c} \sum_{i\,j} \sum_{a'\,c'} \sum_{i'\,j'} \Theta_{(ai)(cj)} \Theta^*_{(a'i')(c'j')} \langle i''\, \alpha_{a''}|\, i\, \alpha_a\rangle\, |\beta_c\, j\rangle \langle \beta_{c'}\, j'|\, \langle i' \alpha_{a'}|\, i''\, \alpha_{a''}\rangle \\ &= \sum_{a\,c} \sum_{i\,j} \sum_{a'\,c'} \sum_{j'} \Theta_{(ai)(cj)} \Theta^*_{(ai)(c'j')} |\beta_c\, j\rangle \langle \beta_{c'} j'| . \end{aligned} \tag{3.28}$$

So,

$$\rho_R = \Theta^T \Theta^*, \tag{3.29}$$

where T and $*$ denote the non-complex-conjugate matrix transpose and complex conjugation, re-

spectively.

We obtain the Schmidt eigenvalues, $\lambda_b^{[2]}$, and eigenstates of L, $|\phi_L^b\rangle$, by diagonalizing ρ_L:

$$|\phi_L^b\rangle = \sum_a \sum_i f^b_{(ai)} |\alpha_a\, i\rangle\,. \tag{3.30}$$

Similarly, we can obtain the Schimdt eigenstates of R, $|\phi_R^b\rangle$, by diagonalizing ρ_R. However, it is more efficient to trace L out in $|\Psi\rangle$:

$$\begin{aligned}
\lambda_b^{[2]} |\phi_R^b\rangle &= \langle\phi_L^b|\,\Psi\rangle \\
&= \sum_{a'} \sum_{i'} \sum_{a\,c} \sum_{i\,j} {f^b_{(a'i')}}^* \Theta_{(ai)(cj)} \langle\alpha_{a'}\, i'|\,\alpha_a\, i\rangle |j\,\beta_c\rangle &(3.31)\\
&= \sum_{a\,c} \sum_{i\,j} {f^b_{(ai)}}^* \Theta_{(ai)(cj)} |j\,\beta_c\rangle\,, &(3.32)
\end{aligned}$$

Since

$$|\phi_R^b\rangle = \sum_c \sum_j g^b_{(cj)} |j\,\beta_c\rangle\,, \tag{3.33}$$

then

$$g^b_{cj} = \sum_a \sum_i \frac{{f^b_{(ai)}}^*}{\lambda_b^{[2]}} \Theta_{(ai)(cj)}. \tag{3.34}$$

In matrix notation,

$$g^b_{cj} = \frac{1}{\lambda_b^{[1]}} \mathrm{diag}\left((f^b)^*\right) \Theta_{(cj)} \tag{3.35}$$

Finally, the time-evolved Γ's are obtained by tracing out the state except for spins 2 and 3:

$$\begin{aligned}
\Gamma'^{[2],i}_{ab} &= \langle\alpha_a|\,\phi_R^b\rangle = g^b &(3.36)\\
\Gamma'^{[3],j}_{bc} &= \langle\phi_L^b|\,\beta_c\rangle = f^b. &(3.37)
\end{aligned}$$

Since the chain is infinite, translationally and flip symmetric, $|\phi_L^b\rangle = |\phi_L^b\rangle$. Hence,

$$\Gamma'^{[2],i}_{ab} = \Gamma'^{[3],j}_{bc} = f^b = g^b. \tag{3.38}$$

3-local Unitary Operators

The generalization of the application of 2-local to 3-local operations is not entirely trivial. See Figure 3.2 for a diagrammatic description of the algorithm.

Details of the Algorithm

The state of the time-evolved system is

$$\begin{aligned}
|\Psi\rangle &= \sum_{a\,b\,c\,d} \sum_{i\,j\,k} \sum_{r\,s\,t} U^{(ijk)}_{(rst)} \lambda_a^{[1]} \Gamma^{[1],r}_{ab} \lambda_b^{[2]} \Gamma^{[2],s}_{bc} \lambda_c^{[3]} \Gamma^{[3],t}_{cd} \lambda_d^{[4]} |a\,i\,j\,k\,d\rangle &(3.39)\\
&= \sum_{a\,d} \sum_{i\,j\,k} \Theta_{(ai)j(dk)} |a\,i\,j\,k\,d\rangle\,, &(3.40)
\end{aligned}$$

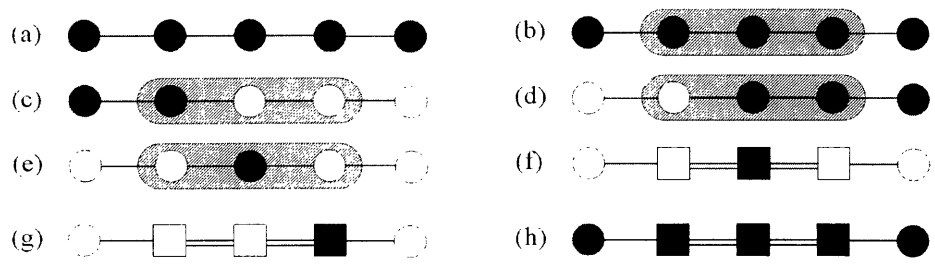

Figure 3-3: Application of a 3-local operator in the MPS representation. (a) Five spins interact locally. The two outermost spins maybe of higher dimensionality in order to capture the state of a longer spin chain. (b) An entangling unitary operator interacts the middle three spins; thus breaking the MPS representation of the state. (c) The three right-most spin states are traced out of the density matrix. (d) Alternatively, we trace out the two left-most spin states. (e) We compute the inner product of the density matrix in d with the reflection of the density matrix in c. We thus obtain the density matrix of the middle spin. (f) We recompute the MPS representation of the middle qubit. (g) The states of the second and fourth spins are found by computing the inner product of the state in f with the state in d. (h) The MPS representation of the interacted spin is reconstructed using the states in f and g.

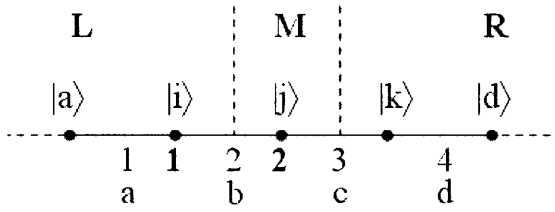

Figure 3-4: Three isolated spins in a spin chain. The letters a,b,c,d label the Schmidt eigenstates of the bonds 1,2,3,4, respectively.

where

$$\Theta_{(ai)j(dk)} = \sum_{bc}\sum_{rst} U^{(ijk)}_{(rst)} \lambda^{[1]}_a \Gamma^{[1],r}_{ab} \lambda^{[2]}_b \Gamma^{[2],s}_{bc} \lambda^{[3]}_c \Gamma^{[3],t}_{cd} \lambda^{[4]}_d. \tag{3.41}$$

In matrix notation,

$$\Theta = U\Lambda^{[1]}\Gamma^{[1]}\Lambda^{[2]}\Gamma^{[2]}\Lambda^{[3]}\Gamma^{[3]}\Lambda^{[4]}. \tag{3.42}$$

The density matrix is

$$\rho = |\Psi\rangle\langle\Psi| \tag{3.43}$$

$$= \sum_{a\,d}\sum_{i\,j\,k}\sum_{a'\,d'}\sum_{i'\,j'\,k'} \Theta_{(ai)j(dk)}\Theta^*_{(a'i')j'(d'k')} |a\,i\,j\,k\,d\rangle\langle a'\,i'\,j'\,k'\,d'|. \tag{3.44}$$

The reduced density matrix for L is

$$\rho_L = \mathrm{Tr}_{MR}(\rho) \tag{3.45}$$

$$= \sum_{d''}\sum_{j''\,k''}\sum_{a\,d}\sum_{i\,j\,k}\sum_{a'\,d'}\sum_{i'\,j'\,k'} \Theta_{(ai)j(dk)}\Theta^*_{(a'i')j'(d'k')} \langle j''\,k''\,d''|\,j\,k\,d\rangle |a\,i\rangle\langle a'\,i'| \langle j'\,k'\,d'|\,j''\,k''\rangle \tag{3.46}$$

$$= \sum_{a\,d}\sum_{i\,j\,k}\sum_{a'}\sum_{i'}\Theta_{(ai)j(dk)}\Theta^*_{(a'i')j(dk)}\,|a\,i\rangle\,\langle a'\,i'|\,. \tag{3.47}$$

In matrix notation,

$$\rho_L = \Theta\Theta^\dagger. \tag{3.48}$$

Here, the elements of the matrix Θ are indexed by $[(ai)][j(dk)]$. Similarly,

$$\begin{aligned}
\rho_R &= \mathrm{Tr}_{ML}(\rho) && (3.49)\\
&= \sum_{a''}\sum_{i''\,j''}\sum_{a\,d}\sum_{i\,j\,k}\sum_{a'\,d'}\sum_{i'\,j'\,k'}\Theta_{(ai)j(dk)}\Theta^*_{(a'i')j'(d'k')}\,\langle a''\,i''\,j''|\,a\,i\,j\rangle\,|k\,d\rangle\,\langle k'\,d'|\,\langle a'\,i'\,j'|\,a''\,i''\,j''\rangle && (3.50)\\
&= \sum_{a\,d}\sum_{i\,j\,k}\sum_{d'}\sum_{k'}\Theta_{(ai)j(dk)}\Theta^*_{(ai)j(d'k')}\,|k\,d\rangle\,\langle k'\,d'|\,. && (3.51)
\end{aligned}$$

In matrix notation,

$$\rho_R = \Theta^T\Theta^*. \tag{3.52}$$

We obtain the eigenstates of L by diagonalizing ρ_L:

$$|\phi^b_L\rangle = \sum_a\sum_i f^b_{(ai)}\,|a\,i\rangle\,. \tag{3.53}$$

Similarly,

$$|\phi^c_R\rangle = \sum_d\sum_k g^c_{(dk)}\,|k\,d\rangle\,. \tag{3.54}$$

We obtain the eigenstates of MR by tracing out L:

$$\begin{aligned}
\lambda^{[2]}_b\,|\phi^b_{MR}\rangle &= \langle\phi^b_L|\,\Psi\rangle && (3.55)\\
&= \sum_{a\,d}\sum_{i\,j\,k}(f^b_{(ai)})^*\Theta_{(ai)j(dk)}\,|j\,k\,d\rangle\,. && (3.56)
\end{aligned}$$

We obtain the eigenstates of M by tracing out R:

$$\begin{aligned}
\lambda^{[3]}_c\,|\phi^{bc}_M\rangle &= \langle\phi^c_R|\,\phi^b_{MR}\rangle && (3.57)\\
&= \sum_j \frac{\mathrm{Tr}\{\mathrm{diag}(f^b)^*\mathrm{diag}(g^c)^*\Theta_j\}}{\lambda^{[2]}_b}\,|j\rangle\,, && (3.58)
\end{aligned}$$

So, the updated Γ for qubit 2 is

$$\Gamma'^{[2],j}_{bc} = \frac{\mathrm{Tr}\{\mathrm{diag}(f^b)^*\mathrm{diag}(g^c)^*\Theta_j\}}{\lambda^{[2]}_b\lambda^{[3]}_c}. \tag{3.59}$$

3.3 An Illustrative Example of MPS

Let us work through a simple example to illustrate the ideas presented in this chapter. In order to build intuition, let us consider the MPS representation of a two spin-1/2 chain in the uniform superposition, i.e. $|\Psi\rangle = (|00\rangle + |01\rangle + |10\rangle + |11\rangle)/2$. By inspection, the MPS representation is given by

$$\lambda^{[1]}_1 = 1; \qquad \lambda^{[1]}_2 = 0;$$

$$\Gamma_a^{[1]i} = \frac{1}{\sqrt{2}} \quad \text{, for } a = 1,2,\ i = 0,1; \qquad \Gamma_a^{[2]j} = \frac{1}{\sqrt{2}}, \text{ for } a = 1,2,\ j = 0,1.$$

We can verify that this representation gives the correct state:

$$\begin{aligned} |\Psi\rangle &= \sum_{i,j=0}^{1} \sum_{a=1}^{2} \Gamma_a^{[1]i} \lambda_a \Gamma_a^{[1]j} |ij\rangle \\ &= \sum_{i,j=0}^{1} \left(\Gamma_1^{[1]i} \lambda_1 \Gamma_1^{[1]j} |ij\rangle + \Gamma_2^{[1]i} \lambda_2 \Gamma_2^{[1]j} |ij\rangle \right) \\ &= \sum_{i,j=0}^{1} \frac{1}{2} |ij\rangle \\ &= \frac{1}{2}(|00\rangle + |01\rangle + |10\rangle + |11\rangle). \end{aligned}$$

3.4 The Cayley Tree

We now move to the description of Cayley trees in the MPS representation. Recall that every spin in a chain has two sets of Schmidt vectors because the spins have two bonds. We conveniently arrange the components of the Schmidt vectors into a matrix Γ_{ab}, where the indices a and b correspond to the two bonds, respectively. In Cayley trees, spins have three interacting bonds. Therefore, we need to arrange the elements of the Schmidt vectors into a 3-rank tensor Γ_{abc}, where the indices a,b, and c correspond to the three bonds connected to the spin. Generalizing the MPS representation in this way, we can write an anzatz for a Cayley tree and compute density matrices and expectation values in a similar fashion.

Expectation Values

Computing the expectation value of an operator on a tree state consists of two steps. First, we need to operate on the state. Second, we need to compute the inner product of the operated state with the original state. More explicitly, we break up the computation of the expectation value of M in the state $|\psi\rangle$, $\langle\psi| M |\psi\rangle$, into computing $|\phi\rangle = M|\psi\rangle$ followed by computing $\langle\psi|\phi\rangle$. We already have the tools to act with local operators. We compute inner products of tree states by succesively tracing over spins and bonds. See Figure 3-5 for a diagrammatic description of this process.

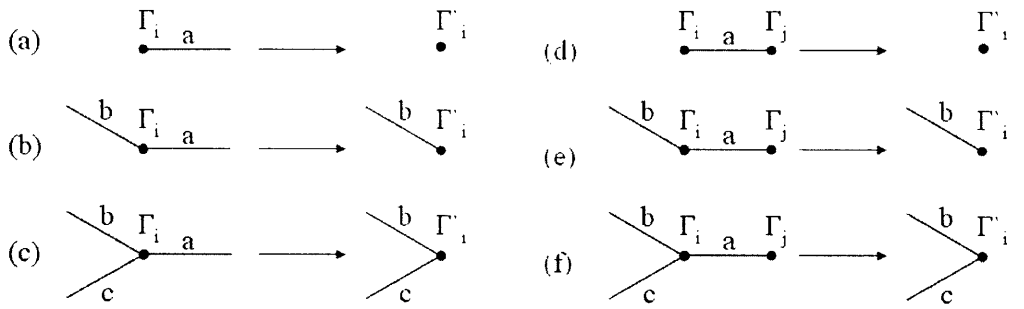

Figure 3-5: Primitive steps in the contraction a graph Cayley tree. Starting from the boundary of the tree, spins and bonds are traced succesively over until a single spin remains. A final trace over the spin states yields the inner product.

Unitary Operations

The interaction of the middle four spins in a rotationally-symmetric Cayley (see Figure 3-7) is fundamental to the efficient algorithm presented in the next section. The interactions of three and two spins in a tree are also necessary. Theoretically, however, the 2- and 3-interactions are special cases of the 4-interaction. Nevertheless, we decided to write code for 2-, 3-, and 4-interactions separately, for reasons of computer performance.

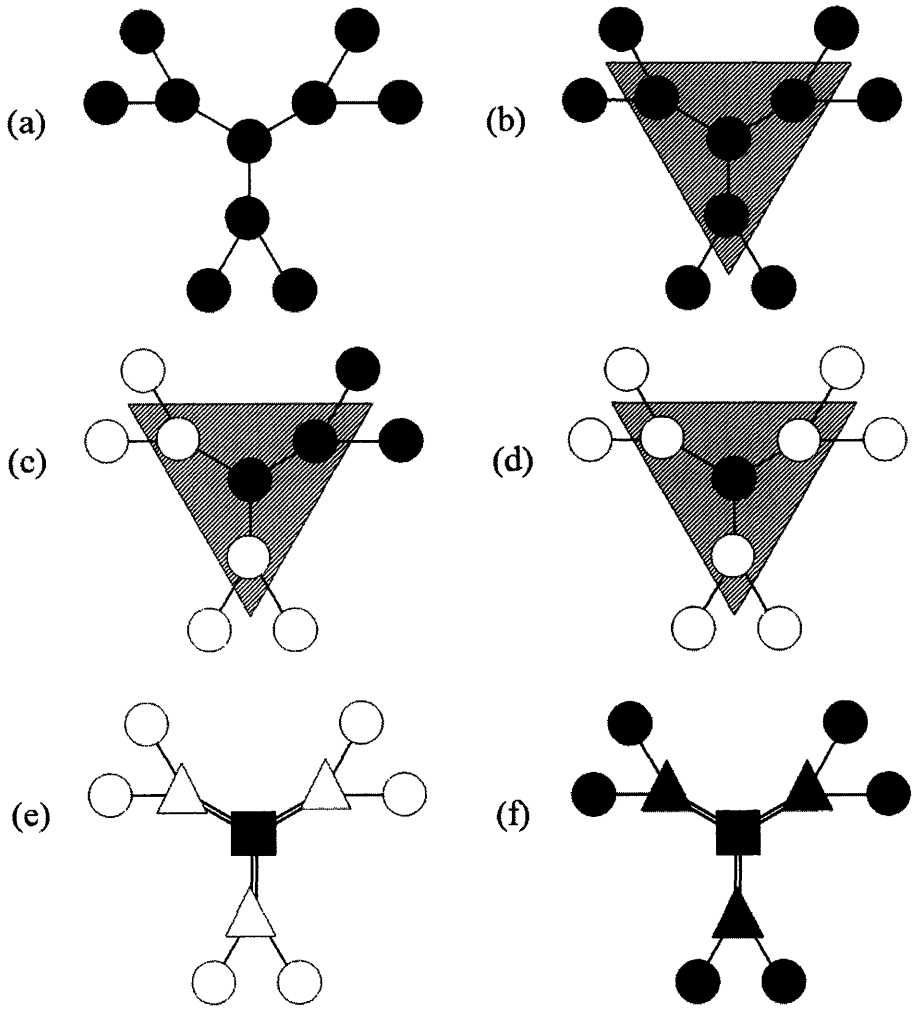

Figure 3-6:

Details of the Algorithm

The wavefunction corresponding to the tree state shown in Figure 3-7 is given by:

$$\begin{aligned} |\Psi\rangle &= \lambda_a^{[1]}\lambda_b^{[2]}\lambda_c^{[2]}\Gamma_{abc}^{[2],j}\lambda_d^{[1]}\lambda_e^{[2]}\lambda_f^{[2]}\Gamma_{def}^{[2],k}\lambda_g^{[1]}\lambda_h^{[2]}\lambda_m^{[2]}\Gamma_{ghm}^{[2],l}\Gamma_{adg}^{[1],i}\,|i\,j\,k\,l\,b\,c\,e\,f\,h\,m\rangle \\ &= \Theta_{i(jbc)(kef)(lhm)}\,|i\,j\,k\,l\,b\,c\,e\,f\,h\,m\rangle\,. \end{aligned}$$

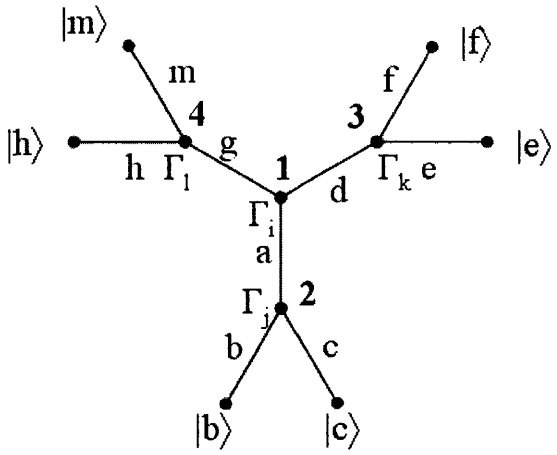

Figure 3-7: The Cayley tree explicitly showing the middle and first level qubits. Every spin and edge have an associated 3-rank tensor Γ and a Schmidt vector, respectively. The elements of these tensors and vectors are combined using the MPS recipe yo yield the wavefunction for the entire tree state.

For convenience, we have omitted the implicit sums over the spins and edges. The density matrix follows immediately:

$$\rho = \Theta_{i(jbc)(kef)(lhm)}\Theta^*_{i'(j'b'c')(k'e'f')(l'h'm')} \left|i\,j\,k\,l\,b\,c\,e\,f\,h\,m\right\rangle \left\langle i'\,j'\,k'\,l'\,b'\,c'\,e'\,f'\,h'\,m'\right| .$$

$$\begin{aligned} \rho_2 &= \mathrm{Tr}_{i\,kef\,lhm}(\rho) \\ &= \Theta_{jbc}\Theta^*_{(j'b'c')} \left|i\,j\,b\,c\right\rangle \left\langle i'\,j'\,b'\,c'\right| \end{aligned}$$

$$\begin{aligned} \rho_1 &= \mathrm{Tr}_{j\,kef\,lhm}(\rho) \\ &= \Theta_i\Theta^*_{i'} \left|i\,j\,b\,c\right\rangle \left\langle i\,j\,b\,c\right| \end{aligned}$$

The eigenstates of the space spanned by the spins $|j\,b\,c\rangle$ are obtained by diagonalizing ρ_2:

$$\left|\Phi^a_2\right\rangle = \sum_{b\,c}\sum_{j} f^a_{(jbc)} \left|j\,b\,c\right\rangle .$$

By symmetry, the eigenstates of the three branches $|\Phi^a_2\rangle = \left|\Phi^d_3\right\rangle = |\Phi^g_4\rangle$ and the eigenvalues $\lambda^{[2]}_a = \lambda^{[3]}_d = \lambda^{[4]}_g$, for $a = d = g$. The updated Γ for the central spin is given by

$$\begin{aligned} \Gamma'^{[1],i}_{adg} &= \frac{1}{(\lambda^{[2]}_a)^3} \left\langle i\,\Phi^a_2\,\Phi^d_3\,\Phi^g_4\right| \Psi\rangle \\ &= \frac{1}{(\lambda^{[2]}_a)^3} (f^a_{jbc})^* (f^d_{kef})^* (f^g_{lhm})^* \Theta_{i(jbc)(kef)(lhm)} . \end{aligned}$$

The updated Γ for spin 2 is given by

$$\Gamma'^{[2],j}_{abc} = \frac{1}{\lambda^{[2]}_a \lambda^{[5]}_b \lambda^{[6]}_c} \left\langle s\,j\,\Phi^d_3\,\Phi^g_4\,b\,c\right| \Psi\rangle ,$$

where $|s\rangle = \lambda_a^{[2]}\lambda_d^{[3]}\lambda_g^{[4]}\Gamma_{adg}^{[1],i}|i\rangle$ is the state of the middle spin. So,

$$\Gamma'^{[2],j}_{abc} = \frac{1}{\lambda_a^{[2]}\lambda_b^{[5]}\lambda_c^{[6]}}\Gamma^{*[1],i}_{adg}(f^a_{kef})^*(f^g_{lhm})^*\Theta_{i(jbc)(kef)(lhm)}.$$

3.5 Efficient Local Operations on Cayley Trees

We are now ready to present a efficient representation for the state of rotationally-symmetric Cayley trees. The key insight is to remember only one branch of the Cayley tree. Since the tree is rotationally-symmetric, all branches are equivalent (see Figure 3-8).

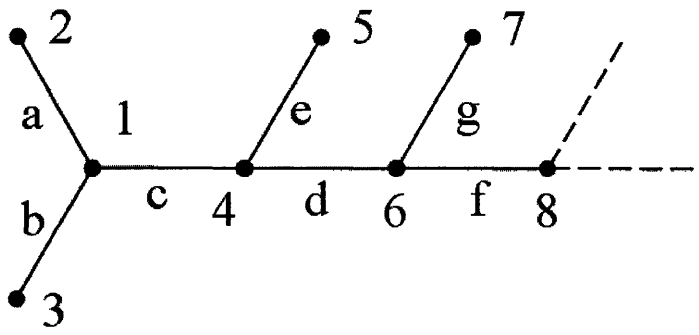

Figure 3-8: A branch of a Cayley tree. Assuming that the operations depend only on the depth of the tree, the states of spins 2,3,4 are equal. Equivalently, the states of spins 5 and 6 are equivalent.

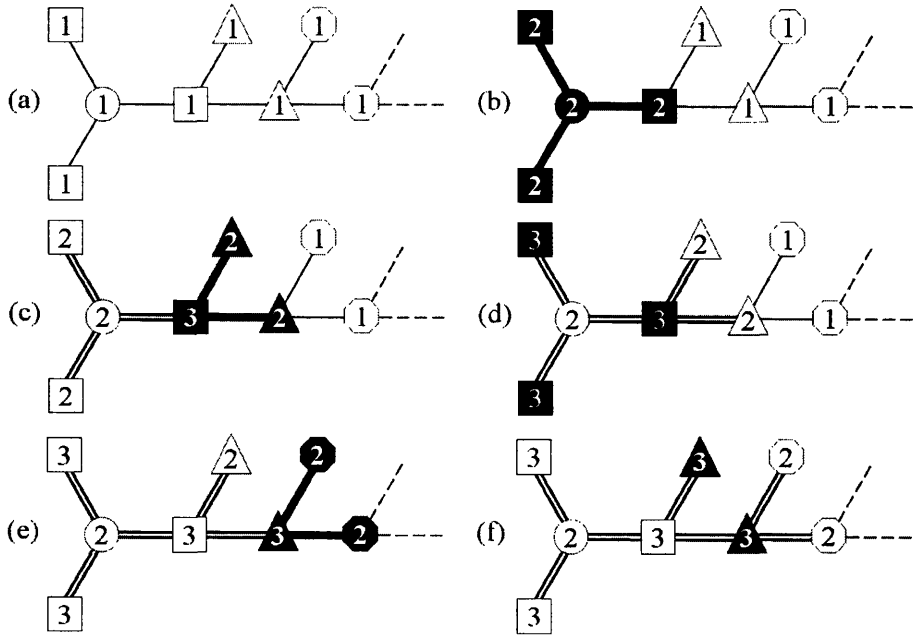

Figure 3-9: Operations on an efficient MPS representation of a Cayley tree. The goal is to interact all bonds once. Single-line represent bonds that have not been interacted while double-lines represent interacted bonds. (a) The state of the spins depends only on the depth. The circle with a number 1 inside represents the state of the middle spin in the first iteration of the algorithm. The square with a 1 represents the state of the spins in the second layer, in the first iteration, and so on. (b) The middle four spins are interacted in the MPS representation. The numbers are increased by 1 to indicate that they correspond to new states. (c) Three spins are interacted. (d) There is a square spin which has interacted all its bonds. Then, we copy the MPS Schmidt tensors and vectors to the other squares. (e) Another set of three spins is interacted. (f) The state of the triangle with all its bonds interacted is copied to the other triangle. We continue this process of interacting three spins and copying MPS parameters until we reach the end of the branch.

Chapter 4

Simulation of Continuous-time Evolution

In this chapter, we approximate the continuous time evolution operator given by the Schödinger equation in terms of a finite sequence of unitary operators. These operators evolve a small number of spins for a small period of time. In order to efficiently evolve states in the MPS representation, we make two approximations. The first approximation involves discretizing time into small intervals. The second approximation exploits the special form of the Hamiltonians which we are interested in. We express unitary operators which act on many spins as a product of local unitaries which act on a small number of spins. This approximation enables us to exploit the power of the MPS representation.

In Section 4.1, we describe the time-discretization approximation. We use the Runge-Kutta method to approximate the solution to the Schödinger equation. In Section 4.2, we explain the Trotter approximation applied to unitary operators.

4.1 The Runge-Kutta Approximation

The Runge-Kutta method is used to approximate the solutions of ordinary differential equations. The Schödinger equation is an linear ordinary first-order operator-valued differential equation. The dynamical quantity is the wavefunction $|\psi(t)\rangle$, which satisfies

$$i\frac{d}{dt}|\psi\rangle = H(t)\,|\psi\rangle\,, \tag{4.1}$$

where $H(t)$ the Hamiltonian, a time-dependent Hermitian operator. The first order Runge-Kutta method approximates the solution to Eq. 4.1 by iterating

$$|\psi(t+dt)\rangle = |\psi(t)\rangle + dt\,H\,|\psi(t)\rangle\,, \tag{4.2}$$

given the initial condition $|\psi(t_0)\rangle = |\psi_0\rangle$. This first-order iteration approximates $|\psi(t)\rangle$ with error $O(dt^2)$. Higher order Runge-Kutta approximations interpolate $|\psi(t)\rangle$ within the interval $[t, t+dt]$.

4.2 The Trotter Approximation

The MPS representation is efficient at applying local operations. The Schödinger time evolution operator given by the Dyson series is a highly non-local operator. Therefore, we wish to find an expression approximately equal to the Dyson series that consists of local operators. Our task is simplified by assuming the following function form for the Hamiltonian:

$$H(s) = (1-s)H_B + sH_P. \tag{4.3}$$

where $s = t/T$, and T is the time scale of the time-evolution. The time-independent Hamiltonian H_B and H_P correspond to the beginning and final (problem) Hamiltonians. In general, these Hamiltonians do not commute. For convenience, we re-arrange the terms in Eq. 4.3:

$$H(s) = H_B + s(H_P - H_B). \tag{4.4}$$

This Hamiltonian has the form $H(t) = A + t/TB$, where A and B are time-independent operators. We derive the first and second order approximations to the Dyson series. The zero-th order approximation is trivial $U(t_0, \Delta t) = 1 + O(\Delta t)$.

We compute approximations to the time-evolution operator Up to first order in Δt, the Dyson series gives

$$\begin{aligned} U(t_0, \Delta t) &= -i \int_{t_0}^{t_0+\Delta t} dt\, H(t) + O(\Delta t^2) \\ &= -i \left(\Delta t A + \frac{\Delta t^2}{2T} B + \frac{\Delta t t_0}{T} B \right). \end{aligned}$$

Matching terms on the left- and right-hand sides yields

$$e^{-iaH_B} e^{-ibH_P} = (1 - iaH_B + O(a^2))(1 - ibH_P + O(b^2)).$$

Solving for the coefficients a and b gives

$$\begin{aligned} a &= (1 - s)\Delta t \\ b &= s\Delta t. \end{aligned}$$

If we expand to second order, we obtain

$$\begin{aligned} e^{-iaH_B} e^{-ibH_P} e^{-icH_B} &= \left(1 - iaH_B - \frac{1}{2}a^2 H_B^2 + O(a^3)\right) \times \\ &\quad \left(1 - ibH_P - \frac{1}{2}b^2 H_P^2 + O(b^3)\right) \times \\ &\quad \left(1 - icH_B - \frac{1}{2}c^2 H_B^2 + O(c^3)\right). \end{aligned}$$

Matching term by term gives the evolution coefficients

$$\begin{aligned} a &= c = \frac{\Delta t}{2}\left(1 - s - \frac{\Delta t}{2T}\right) \\ b &= s\Delta t + \frac{\Delta t^2}{2T}. \end{aligned}$$

4.3 Quantum Adiabatic Time Evolution

We have developed the necessary tools to efficiently simulate the time-evolution of spin networks with Quantum Adiabatic Evolution Hamiltonians of the form $H(s) = (1 - s)H_B + sH_P$. Let us summarize the algorithm to approximately simulate the evolution $U(t_0, t_f)\,|\psi\rangle$:

1. Discretize the time interval $[t_0, t_f]$ into sub-intervals $[t_i, t_i + \Delta t]$ of length Δt. We can then write $U(t_0, t_f) = U(t_i, t_i + \Delta t)U(t_i + \Delta t, t_i + 2\Delta t) \ldots U(t_f - \Delta t, t_f)$.

2. For each time interval Δt, expand the time-evolution operator $U(t, t + \Delta t)$ using the Dyson series.

3. Express each operator term in the Dyson series as a sequence of local non-communiting operators.

4. Act with the local operators on $|\psi\rangle$, restoring the MPS representation in each iteration.

Chapter 5

Simulation Results

We simulated the time-evolution of two quantum adiabatic Hamiltonians. The AGREE on a spin chain problem corresponds to the Hamiltonian

$$H_{AGREE}(s) = (1-s)\sum_i \sigma_X^{(i)} + s\sum_i \sigma_Z^{(i)}\sigma_Z^{(i+1)}. \tag{5.1}$$

The FAVORITE on a spin chain problem is a generalization to the AGREE problem. The FAVORITE Hamiltonian is

$$H_{FAVORITE}(s) = (1-s)\sum_i \sigma_X(i) + s\sum_i \sigma_Z^{(i)}\sigma_Z^{(i+1)} + \epsilon\,|ij=11\rangle\langle ij=11|\,. \tag{5.2}$$

The FAVORITE Hamiltonian reduces to AGREE for $\epsilon = 0$. For $\epsilon = 2$, the FAVORITE Hamiltonian is effectively a 1-local Hamiltonian that can be solved exactly analytically.

5.1 The Spin Chain

Figure 5-1 shows the two Schmidt eigenvalues corresponding to the middle bond in a spin chain of 10 spins. In the beginning of the evolution, the state is in the uniform superposition. The two eigenvalues meet near $s = 0.6$ and then they oscillate about $1/\sqrt{2}$. Since the time of evolution is finite, the evolution is not strictly adiabatic. So, the oscillations of the eigenvalues are contributions from spin waves. The state at $s = 1$ corresponds to the "cat" state

$$|\psi(s=1)\rangle \quad = \quad 1/\sqrt(2)(|00\ldots0\rangle + |11\ldots1\rangle).$$

Figure 5-2 shows the expectation value of the energy of the spin chain discussed before. Several evolutions were performed with various T. As T increases, the final energy decreases because the evolution becomes more adiabatic.

Figure 5-3 shows the probablity that the state is in the final "cat" state in a spin chain. In the beginning of the evolution, the chain is in the uniform superposition. So, the probability is in the order of 2^{-20}. However, as the evolution approaches $s = 1$, the probability of success approaches 1.

Figure 5-4 shows the Schmidt eigenvalues corresponding to the middle bonds of a spin chain with a FAVORITE problem Hamiltonian. For $\epsilon = 0$, the eigenvalues match that of the AGREE problem. As ϵ is dialed to $\epsilon = 2$, the eigenvalues aproach 1 and 0. The Hamiltonian is 1-local for $\epsilon = 2$. Thus, we expect that the time evolution does not entangle the spins. This is in fact the case because the Schmidt eigenvalues, which provide a measure for entanglement, remain close to $[1, 0]$ for ϵ close to 2 throughout the evolution.

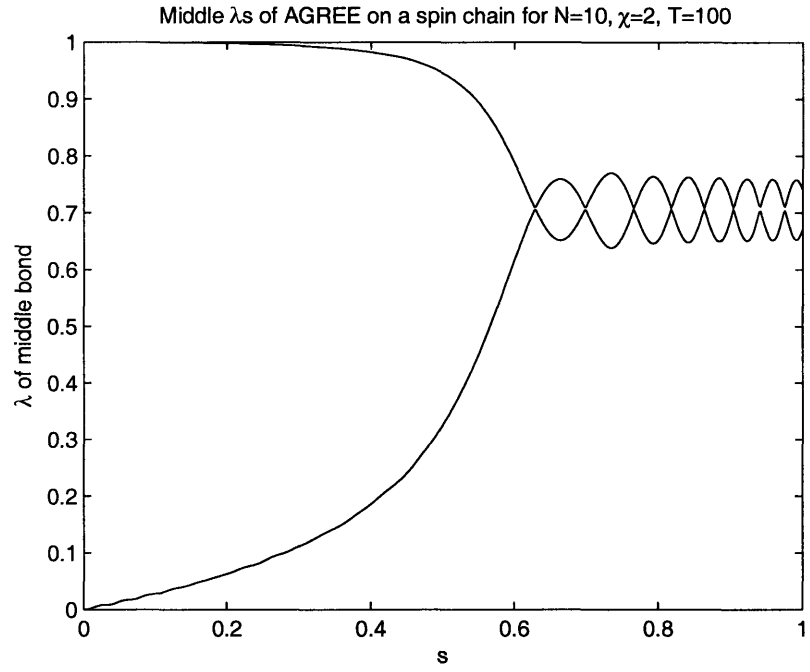

Figure 5-1: Lambda of middle bonds of AGREE on a spin chain. The parameters are $dt = 0.01$, $N = 10$,$\chi = 2$, and $T = 100$.

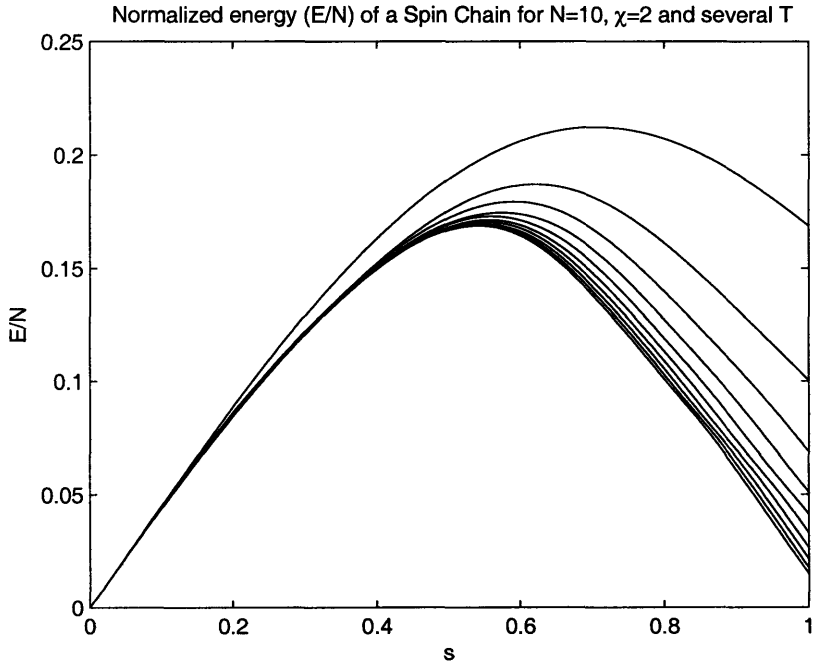

Figure 5-2: Normalized energy of AGREE on a spin chain for running times T. The parameters are $dt = 0.01$,$N = 10$,$\chi = 2$, and $T = 5 : 5 : 60$.

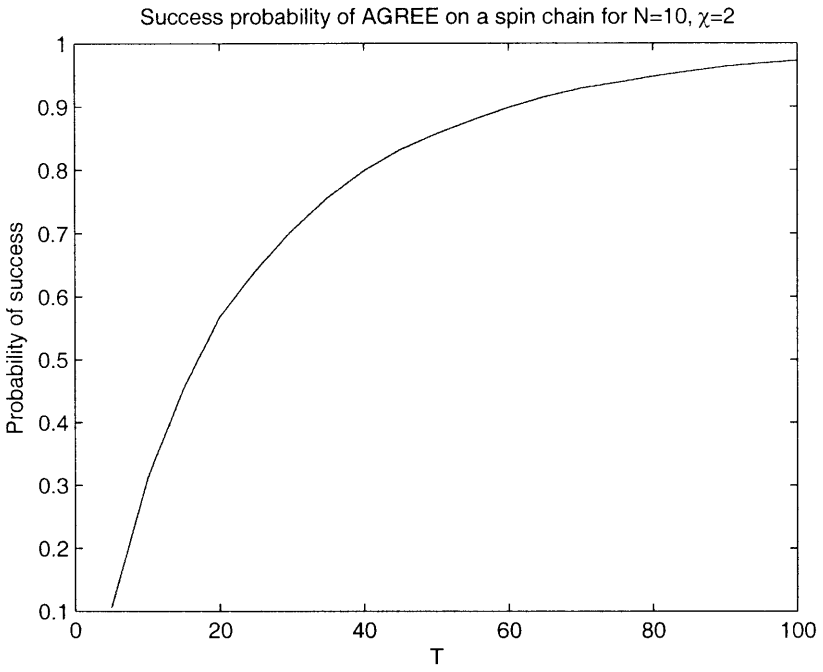

Figure 5-3: Probability of success of AGREE on a spin chain as a function of the running time T. The parameters are $dt = 0.01, N = 10, \chi = 2$.

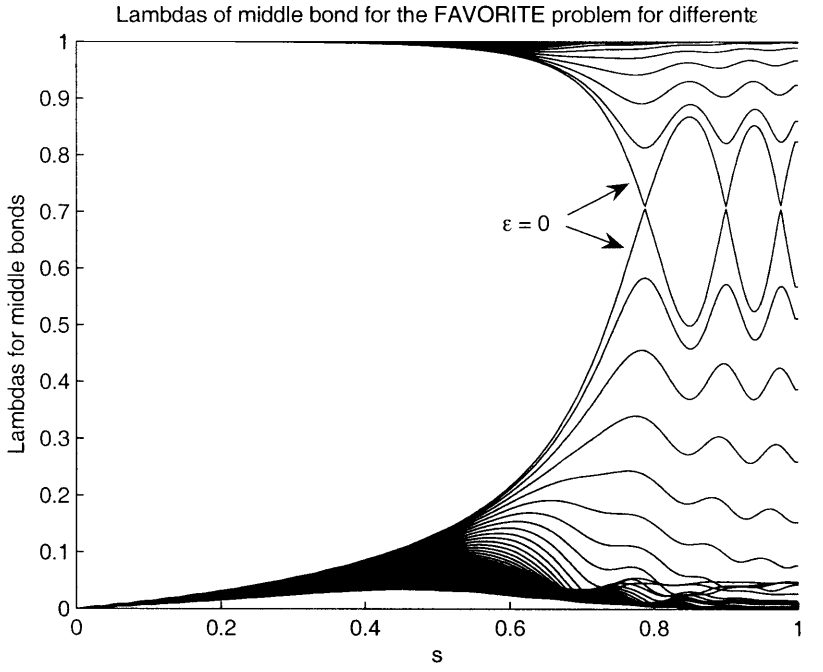

Figure 5-4: Lambdas of middle bonds of instances of the FAVORITE problem on a spin chain for different ϵ. The parameters are $T = 50$, $dt = 0.1$, $X = 2$, $\epsilon = 0 : .02 : 1$.

5.2 The Cayley Tree

Figure 5-5 shows the expected energy in a Cayley tree 20 levels deep. The system was evolved from an X-field Hamiltonian to the AGREE problem Hamiltonian in $T = 4$. Figure 5-6 the Schmidt eigenvalues corresponding to bonds at different levels. The eigenvalues near the center of the tree most closely match the eigenvalues of a spin chain whereas the eigenvalues closer the boundary tend to collapse to 1 and 0.

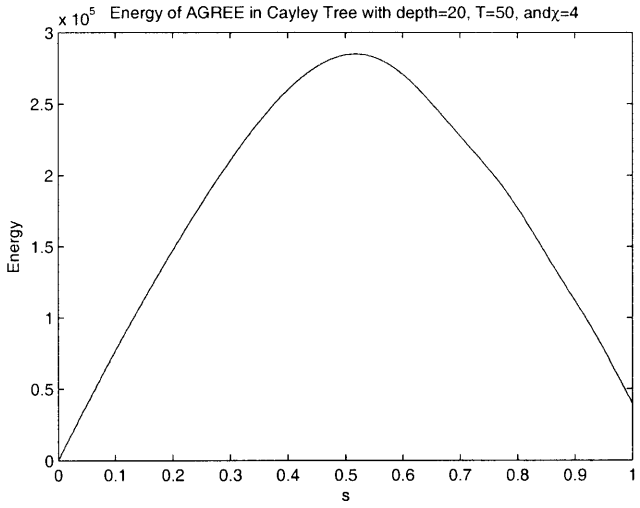

Figure 5-5: Energy of AGREE on a Cayley tree. The parameters are $d = 20$,$T = 50$,$chi = 4$.

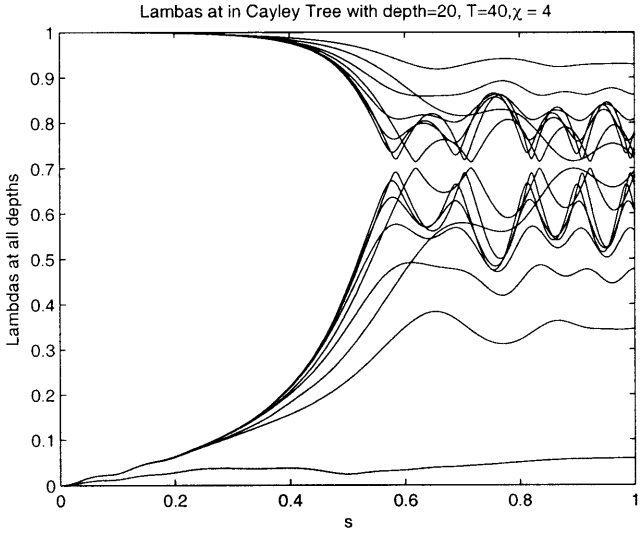

Figure 5-6: Lambdas of AGREE on a Cayley tree for different depths. The parameters are $d = 20$,$T = 40$,$\chi = 4$.

Chapter 6

Conclusions and Future Work

We have introduced the Matrix Product State representation in the context of spin chains and Cayley trees. The symmetry of the Cayley tree was exploited to approximately represent the state of a Cayley tree using poly(d) parameters, where d is the depth of the tree. The exact representation uses $O(2^{3^d})$ parameters.

There are many paths to improve and extend the results of this thesis. For example, the compact representation of trees could be extended to other topologies such as 4-trees or honeycombs. The key insight is to find and exploit the symmetry of those systems to reduce the number of parameters in the representation.

We explicitly computed the time-evolution of spin networks. However, if we restrict ourselves to computing only the exact ground state energy then imaginary-time evolution has advantages to out current approach. Given any[1] state in the Hilbert space, imaginary-time evolution finds the ground state of the instantaneous Hamiltonian. Therefore, we can study the adiabatic behavior of Hamiltonians without explicitly simulating the time-evolution. A clear problem in implementing imaginary-time evolution is the Trotter expansion. Since the imaginary-time evolution operator is no longer unitary, the Trotter expansion is not valid. Thus, an alternate expansion of the evolution operator is needed.

[1] A necessary condition is that the state has a nonzero overlap with the ground state.

Bibliography

[1] Dorit Aharonov, Wim van Dam, Julia Kempe, Zeph Landau, Seth Lloyd, and Oded Regev. Adiabatic quantum computation is equivalent to standard quantum computation, 2004.

[2] M. C. Banuls, R. Orus, J. I. Latorre, A. Perez, and P. Ruiz-Femenia. Simulation of many-qubit quantum computation with matrix product states. *Physical Review A*, 73:022344, 2006.

[3] A. J. Daley, C. Kollath, U. Schollwoeck, and G. Vidal. Time-dependent density-matrix renormalization-group using adaptive effective hilbert spaces. *THEOR.EXP.*, page P04005, 2004.

[4] Edward Farhi, Jeffrey Goldstone, Sam Gutmann, and Michael Sipser. Quantum computation by adiabatic evolution, 2000.

[5] J. I. Latorre, E. Rico, and G. Vidal. Ground state entanglement in quantum spin chains. *QUANT.INF.AND COMP.*, 4:048, 2004.

[6] Tobias J. Osborne and Michael A. Nielsen. Entanglement, quantum phase transitions, and density matrix renormalization, 2001.

[7] Ulrich Schollwoeck. Time-dependent density-matrix renormalization-group methods. *J.PHYS.SOC.JPN*, 246, 2005.

[8] F. Verstraete, D. Porras, and J. I. Cirac. Dmrg and periodic boundary conditions: a quantum information perspective. *Physical Review Letters*, 93:227205, 2004.

[9] G. Vidal. Efficient simulation of one-dimensional quantum many-body systems. *Physical Review Letters*. 93:040502, 2004.

[10] Guifre Vidal. Efficient classical simulation of slightly entangled quantum computations. *Physical Review Letters*, 91:147902, 2003.